


Taxifolin prevents postprandial hyperglycemia by regulating the activity of α -amylase: Evidence from an *in vivo* and *in silico* studies

Kanwal Rehman¹ | Tahir Ali Chohan² | Iqra Waheed¹ | Zeeshan Gilani³ | Muhammad Sajid Hamid Akash⁴ 

¹Institute of Pharmacy, Physiology and Pharmacology, University of Agriculture, Faisalabad, Pakistan

²Institute of Pharmaceutical Sciences, University of Veterinary and Animal Sciences, Lahore, Pakistan

³Department of Computer Science, COMSATS Institute of Information Technology, Lahore, Pakistan

⁴Department of Pharmaceutical Chemistry, Faculty of Pharmaceutical Sciences, Government College University, Faisalabad, Pakistan

Correspondence

Muhammad Sajid Hamid Akash,
Department of Pharmaceutical Chemistry, Faculty of Pharmaceutical Sciences, Government College University, Faisalabad, Pakistan.
Email: sajidakash@gcuf.edu.pk; sajidakash@gmail.com

Abstract

There has been a dramatic increase in the prevalence of diabetes mellitus (DM) and its associated complications globally. The postprandial stage of DM involves prompt elevation in the levels of blood glucose and α -amylase, a carbohydrate-metabolizing enzyme is mainly involved in the regulation of postprandial hyperglycemia. This study was designed to assess the ability of a well-known flavonoid, taxifolin (TFN), against postprandial hyperglycemia and its inhibitory effects on α -amylase activity through the assessment of therapeutic potentials of TFN in an alloxan-induced diabetic animal model. The binding potential TFN with an α -amylase receptor was also investigated through molecular dynamics (MD) simulation and docking of to compare the binding affinities and energies of TFN and standard drug acarbose (ACB) with target enzyme. TFN significantly improved the postprandial hyperglycemia, lipid profile, and serum levels of α -amylase, lipase, and C-reactive protein in a dose-dependent manner when compared with that of either DM-induced and ACB-treated alloxan-induced diabetic rats. Moreover, TFN also enhanced the anti-oxidant status and normal functioning of the liver in alloxan-induced diabetic rats more efficiently as compared to that of ACB-treated alloxan-induced diabetic rats. Therapeutic potentials of TFN were also verified by MD simulation and docking results, which exhibited that the binding energy and affinity of TFN to bind with receptor was significantly higher as compared to that of ACB. Hence, the results of this study signify that TFN might be a potent inhibitor of α -amylase that has the potential to regulate the postprandial hyperglycemia along with its anti-inflammatory and anti-oxidant properties during the treatment of DM.

KEYWORDS

diabetes mellitus (DM), molecular docking, molecular dynamics (MD) simulation, taxifolin (TFN)

Kanwal Rehman, Tahir Ali Chohan, and Iqra Waheed contributed equally in this work.

1 | INTRODUCTION

Type 2 diabetes mellitus (T2DM) is a metabolic disorder having an abnormally high level of blood glucose because of dysregulation of insulin secretion from β -cells of pancreatic islets, insulin resistance in peripheral tissues, decreased glucose uptake in peripheral tissues, and/or abnormal hepatic glucose production and carbohydrate metabolism.¹⁻³ It has been estimated that due to the increased incidences of T2DM by the year 2030, there will be a drastic increase in the global health burden in terms of prevalence of T2DM and its associated complications. There are numerous causative factors for the development of T2DM. One of the endogenous factors that regulate glucose metabolism is a carbohydrate-metabolizing enzyme, namely, α -amylase. Postprandial hyperglycemia is one of the main reasons for the induction of many diabetic complications.⁴ Among which the cardiovascular diseases are the major complications that are associated with T2DM and are rapidly prevailing globally.⁵ This calls for a well-time management of hyperglycemia for the prevention of DM-associated complications.⁶

α -amylase is a carbohydrate-metabolizing enzyme that contributes in increasing the level of glucose in blood.^{7,8} Similarly, insulin influentially secreted from the β -cells of pancreatic islets soon after the glucose metabolism by carbohydrate digestion by α -amylase results in the exhaustion of β -cells.⁹ Correspondingly, inhibin of these carbohydrate-digesting enzymes, that is, α -amylase can prove to be a suitable option for the treatment of DM.¹⁰ As modern research is elucidating the increasingly associated adverse events of commercially available antidiabetic drugs,¹¹ there is a strong need for exploring and detecting the other ways of ideal therapeutics for DM treatment showing maximum efficacy and minimal side effects. Relating to the therapeutic choices available for the treatment and prevention of DM, there are many commercial drugs available such as acarbose (ACB). ACB is one of the standard drugs that is the potent inhibitor of α -amylase and α -glucosidase. By inhibiting these enzymes, ACB decreases the absorption of carbohydrates from the intestine and is exclusively used for the treatment and/or prevention of T2DM.¹² However, these drugs are known to show many unwanted effects like diarrhea, lactic acidosis, liver toxicity, and cardiovascular complications.^{11,13}

Flavonoids can meet this criterion of an ideal therapeutics while combating against DM and its associated complications.^{8,14,15} Among various types of flavonoids, taxifolin (TFN), also known as dihydroquercetin, is known to have therapeutic potentials against various types of diseases.¹⁶ In early studies, TFN has shown to protect the

hyperglycemia-induced osmotic stress by inhibiting the accumulation of recombinant human aldose reductase and sorbitol in humans.¹⁷ As the anti-oxidant potential of TFN is concerned, recently this property of TFN has shown to protect the heart and vascular tissues through providing the protection against lipid peroxidation and reducing the incidences of apoptosis.¹⁸ However, the probable beneficial properties of TFN on inhibition of α -amylase remains so far to be elucidated.

Thereby, the purpose of this study was to investigate the inhibitory effects of TFN in comparison to a well-known inhibitor of α -amylase, that is, ACB on the activity of α -amylase in vivo using an experimentally induced diabetic animal model. Moreover, the associated biochemical parameters including serum levels of glucose, insulin, liver, and kidney function biomarkers along with serum levels of anti-oxidant enzymes were also investigated. Furthermore, we also performed molecular dynamics (MD) simulation and protein docking to compare the binding efficacy of TFN and ACB with α -amylase enzyme to verify the therapeutic effects TFN and ACB attained by performing experimental studies.

2 | MATERIALS AND METHODS

2.1 | Animals and treatment protocol

All studies using experimental animals were conducted in accordance with the Institutional Biosafety Committee, University of Agriculture, Faisalabad, Pakistan, for the use of laboratory animals. Thirty healthy albino rats of either sex having approximate body weight of 200 to 250 g were taken and kept in cages in animal room of the Institute of Pharmacy, Physiology and Pharmacology, University of Agriculture, Faisalabad, Pakistan. Rats were given standard basal diet and provided with water ad libitum at room temperature ($22 \pm 2^\circ\text{C}$) for 12 h light and 12 h dark cycle. After one week of acclimatization, rats were divided into five groups. Group 1 was nondiabetic control (NDC). Group 2 was alloxan-induced nontreated diabetic control (DC) through a single intraperitoneal injection of alloxan (120 mg/kg body weight of rat). Group 3 was alloxan-induced diabetic rats treated with ACB (40 mg/kg) through the intragastric route. Group 4 was alloxan-induced diabetic rats treated with 25 mg/kg of taxifolin (LD-TFN) through the intragastric route. Group 5 was alloxan-induced diabetic rats treated with 100 mg/kg of taxifolin (HD-TFN) through the intragastric route. The treatment was carried out for one month. Blood glucose was measured using a glucometer (Accu check Performa, Roche Pakistan Limited) at day 1 for basal values followed by the measurement at day 3 for the confirmation of diabetes in alloxan-treated groups.

2.2 | Sample collection

Blood samples were collected from rat's tail. Collected blood samples were allowed to coagulate at room temperature for 20 min. Later, blood was centrifuged for 15 min at 3000 × g. The serum collected after centrifugation was stored at −20°C until further analysis.

2.3 | Impact of treatment on the blood glucose level

Hyperglycemia reflects the increase in the blood glucose level and is one of the key indicators of DM; therefore, glucometer (Accu check Performa) was used to measure the blood glucose levels in all groups of experimental animals.

2.4 | Impact of treatment on amylase activity

To estimate the impact of alloxan and treatment (ACB, LD-TFN, and HD-TFN) on carbohydrate metabolism in collected samples of experimental animals, the serum level of α -amylase was measured before (1st day), during (15th day), and last (30th day) day of the treatment period.

2.5 | Impact of treatment on lipase activity

To evaluate the impact of alloxan and treatment (ACB, LD-TFN, and HD-TFN) on lipid metabolism in collected samples of experimental animals from all groups, the serum level of lipase was measured quantitatively using an assay kit at predefined time points, that is, before, during, and last day of the treatment period.

2.6 | Assessment of treatment on lipid profile

To estimate the impact of alloxan and treatment (ACB, LD-TFN, and HD-TFN) on the lipid profile, the serum levels of high density lipoprotein (HDL), total cholesterol (TC), triglycerides (TGs), and low density lipoproteins (LDL) were measured using their corresponding assay kits at predefined time points, that is, before, during, and last day of the treatment period.

2.7 | Impact of treatment on anti-oxidant enzyme status

To estimate the impact of alloxan and treatment (ACB, LD-TFN, and HD-TFN) on the anti-oxidant enzyme

status in collected samples of experimental animals from all groups, serum levels of superoxide dismutase (SOD) and catalase (CAT) were measured quantitatively using their corresponding assay kits at predefined time points, that is, before, during, and last day of the treatment period.

2.8 | Impact of treatment on inflammatory biomarkers

To estimate the impact of alloxan and treatment (ACB, LD-TFN, and HD-TFN) on inflammation, the serum levels of C-reactive protein (CRP) and white blood cells (WBCs) count were measured at predefined time points.

2.9 | Impact of treatment on liver function

To estimate the impact of alloxan and treatment on the liver in collected samples of experimental animals from all groups, the serum levels of aspartate aminotransferase (AST) and alanine aminotransferase (ALT) were measured using their corresponding assay reagent kits at 1st, 15th, and last (30th) day of the treatment period.

2.10 | Computational and docking studies

2.10.1 | Ligand preparation and docking studies

At first, the cocrystal structures of α -amylase, ACB, and catechin (PDB entry: 2QV4, 3BC9, and 4C94, respectively¹⁹⁻²¹) were retrieved from RCSB protein data bank (PDB) (Figure 9A and Figure 1S, supporting information). The geometrically active conformation of catechin was extracted from 4C94 to be used as a template to build the structure of TFN. Finally, a 3-D-structure of TFN was constructed using a Sybyl-X1.3/ SKETCH module²² by minor modification at 4-position of ring-C (Figure 1S, supporting information). Three-dimensional structures of both compounds (ACB and TFN) were minimized by Tripos force field with Gasteiger-Hückel atomic charge. Flexible docking simulations were carried out to investigate the binding modes of selected inhibitors in complex with α -amylase using a Surflex-Dock module of molecular modeling software package SYBYL-X 1.3.²³ The crystal structures of complex α -amylase with modified ACB (PDB entry: 2QV4¹⁹), downloaded from RCSB-PDB, were used as a starting point for further calculations. Structure of α -amylase was carefully analyzed to confirm the chemical accuracy using structure preparation tools implemented in a biopolymer module of SYBYL-X 1.3.²² Missing hydrogens were added, charges were applied, and atom types were assigned according to the

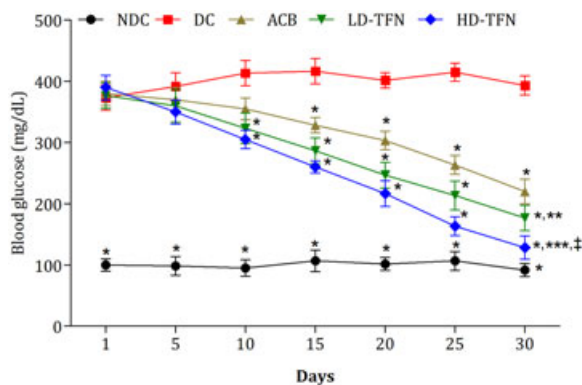


FIGURE 1 Effect of treatment on glycemia. Treatment was started after the induction of diabetes mellitus. Normal saline was administered in nondiabetic rats ($n = 5$) and alloxan-induced diabetic rats ($n = 5$) once a day. ACB (40 mg/kg), LD-TFN (25 mg/kg), and HD-TFN (100 mg/kg) were administered once a day in ACB, LD-TFN, and HD-TFN groups, respectively. Blood glucose was measured once in a week. The level of significant difference was estimated by Bonferroni post-test using two-way ANOVA. $*P < 0.001$ when compared with the NDC group. $**P < 0.001$ when compared with the DC group. $^{\circ}P < 0.05$ when compared with the ACB group. $^{***}P < 0.001$ when compared with the ACB group. $^{\ddagger}P < 0.001$ when compared with the DC group. ACB, acarbose; ANOVA, analysis of variance; DC, diabetic control; HD-TFN, high-dose taxifolin; LD-TFN, low-dose taxifolin; n, total number of animals used in each group

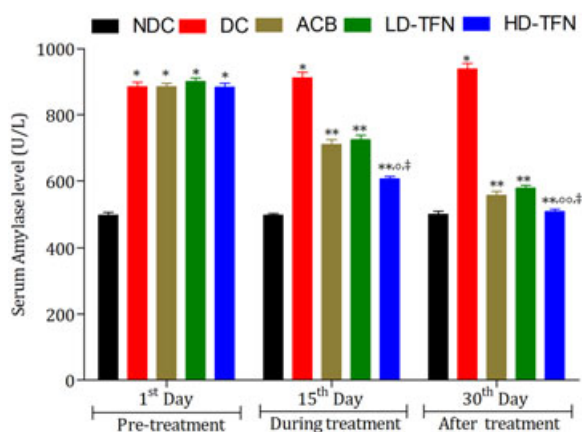


FIGURE 2 Effect of treatment on the amylase activity. To estimate the impact of alloxan and treatment (ACB, LD-TFN, and HD-TFN) on carbohydrate metabolism, the serum levels of amylase were measured at 1st, 15th, and last (30th) day of the treatment period. The level of significant difference was estimated by Bonferroni post-test using two-way ANOVA. $*P < 0.001$ when compared with the NDC group. $**P < 0.001$ when compared with the DC group. $^{\circ}P < 0.001$ when compared with the ACB group. $^{\circ\circ}P < 0.05$ when compared with the ACB group at the 30th day of the treatment period. $^{\ddagger}P < 0.001$ when compared with the LD-TFN group. ACB, acarbose; ANOVA, analysis of variance; DC, diabetic control; HD-TFN, high-dose taxifolin; LD-TFN, low-dose taxifolin; n, total number of animals used in each group; NDC, nondiabetic control

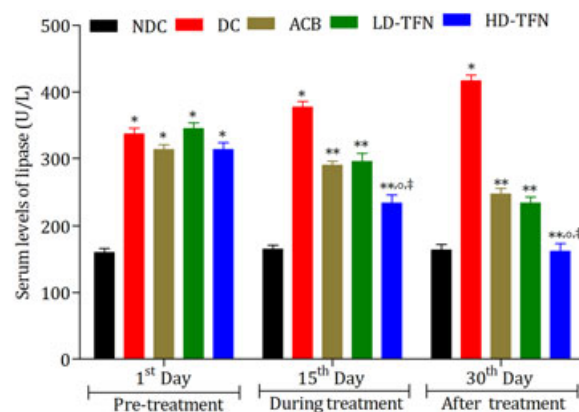


FIGURE 3 Effect of treatment on lipase. To estimate the impact of alloxan and treatment (ACB, LD-TFN, and HD-TFN) on lipid metabolism, the serum levels of lipase were measured at 1st, 15th, and last (30th) day of the treatment period. The level of significant difference was estimated by Bonferroni post-test using two-way ANOVA. $*P < 0.001$ when compared with the NDC group. $**P < 0.001$ when compared with the DC group. $^{\circ}P < 0.001$ when compared with the ACB group. $^{\ddagger}P < 0.001$ when compared with the LD-TFN group. ACB, acarbose; ANOVA, analysis of variance; DC, diabetic control; HD-TFN, high-dose taxifolin; LD-TFN, low-dose taxifolin; n, total number of animals used in each group; NDC, nondiabetic control

AMBER 7 FF99 force field. Finally, the energy was minimized to prevent the steric clashes using the Powell algorithm with a convergence gradient of 0.5 kcal/(mol·Å) for 1000 cycles. The primary conformation of modified ACB in 2QV4 was used as the starting point for ProtoMol generation (an idealized active site). Finally, the generated conformations of ACB and TFN were individually docked into the active site of α -amylase (2QV4) to replace modified ACB. Twenty best-docked poses were finally saved for each inhibitor. These putative poses of ligand were ranked using the Hammerhead scoring function.^{24,25} Surflex dock module employs an empirically derived consensus scoring (C -score) function that combines Hammerhead's empirical scoring function,^{24,25} that is, D -score (dock score), G -score (gold score), Chem-Score, potential mean force score, and the total score with a molecular similarity method (morphological similarity) to generate and rank putative poses of ligand fragments. Each of the ligands was docked into the active site of a receptor at least ten times, and 20 highest ranked putative poses according to the Hammerhead scoring (C -score) function were finally saved for each inhibitor. The top-ranking docking conformations for each compound were retrieved for further MD simulations.

2.10.2 | Molecular dynamics simulations

The final complexes of ACB and TFN bond to the α -amylase were subjected to the MD simulations for

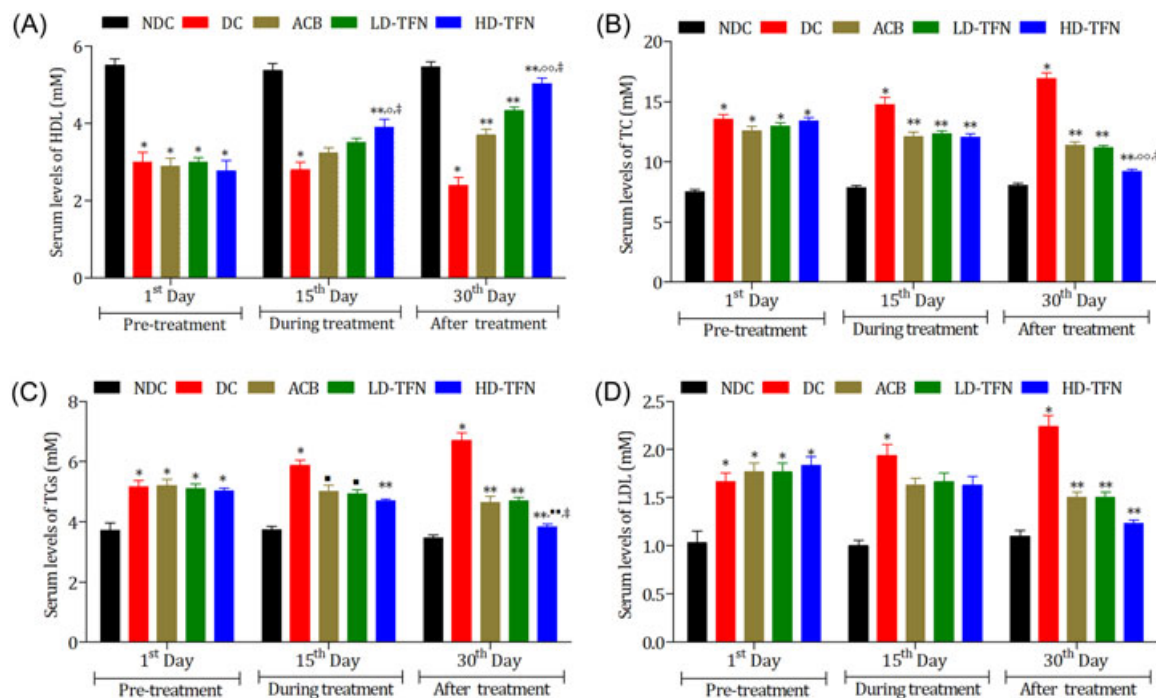


FIGURE 4 Effect of treatment on the lipid profile. To estimate the impact of alloxan and treatment (ACB, LD-TFN, and HD-TFN) on the lipid profile, the serum levels of HDL (A), TC; (B), TGs; (C), and LDL; (D), were measured at 1st, 15th, and last (30th) day of the treatment period. The level of significant difference was estimated by Bonferroni posttest using two-way ANOVA. * $P < 0.001$ when compared with the NDC group. ■ $P < 0.01$ when compared with the DC group. ** $P < 0.001$ when compared with the DC group. ■■ $P < 0.01$ when compared with the ACB and LD-TFN group. ° $P < 0.05$ when compared with the ACB group. °° $P < 0.001$ when compared with the ACB group. † $P < 0.05$ when compared with the LD-TFN group. ACB, acarbose; ANOVA, analysis of variance; DC, diabetic control; HDL, high density lipoprotein; HD-TFN, high-dose taxifolin; LDL, low density lipoproteins; LD-TFN, low-dose taxifolinn; n, total number of animals used in each group; NDC, nondiabetic control; TC, total cholesterol; TGs, Triglycerides

further stabilization and refinement. All MD simulations were thoroughly performed in AMBER16 software package²⁶ at least for 50 nanoseconds (ns). Both systems were neutralized by replacing some water molecules with Na^+ counter-ions. The force field parameters for protein-ligand complexes were assigned using AMBER ff99SB²⁷ force field for protein while general AMBER force field²⁸ (GAFF together with RESP charges²⁹) for ligands. Each system was relaxed at 300 K and 1 bar pressure in explicit TIP3P by executing three consecutive steps of energy minimization before a solvation model.³⁰ Keeping in account the system stability, MD equilibrations were performed in additional eight steps for each system.³¹ Finally, each system was subjected to MD simulation using NPT ensemble at constant temperature and pressure of 300 K and 1 atm, respectively.³² The coordinates of MD simulation trajectories were collected at every 1 and 2 ps during equilibration and MD production run, respectively. All MD simulations procedures were carried out using CARNAL, ANAL, and CPPTRAJ modules of AMBER16.

2.10.3 | Free energy calculation

Molecular mechanics-based scoring method MM/PB (GB)SA,³³ in AMBER16 software package, was applied to compare the binding-free energies of selected compounds in α -amylase complexes. At first, the representative sets of equilibrium confirmations for complex, free receptor, and free ligand were prepared and binding-free energy was calculated as a difference between the total free energy of ligand-protein complex (G_{com}) and sum of individual receptor (G_{rec}) and ligands (G_{lig}) free energy. At least, 1000 snapshots for each complex (ACB- and TFN- α -amylase), were taken from the last 5 ns stable MD trajectory at 5 ps intervals to predict the binding-free energies (ΔG_{bind}).

3 | RESULTS

3.1 | Effect of treatment on glycemia

Hyperglycemia means the increase in the level of blood glucose and is considered as a hallmark of DM. To

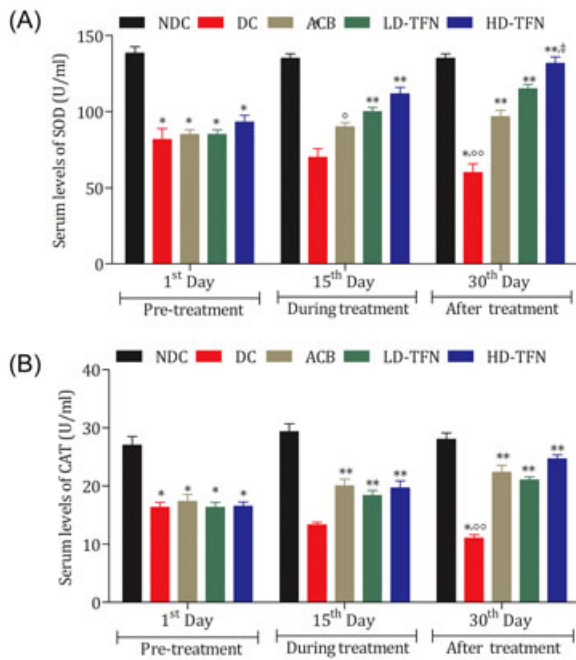


FIGURE 5 Effect of treatment on the anti-oxidant status. To estimate the impact of alloxan and treatment (ACB, LD-TFN, and HD-TFN) on the anti-oxidant status, the serum levels of SOD (A), and CAT (B), were measured using their corresponding assay reagent kits at 1st, 15th, and last (30th) day of the treatment period. The level of significant difference was estimated by Bonferroni post-test using two-way ANOVA. * $P < 0.0001$ when compared with the NDC group. ** $P < 0.001$ and ° $P < 0.01$ when compared with the DC group. † $P < 0.001$ when compared with the ACB group at the 30th day of the treatment period. °° $P < 0.001$ when compared with the DC group at the 30th day of the treatment period. ACB, acarbose; ANOVA, analysis of variance; CAT, catalase; DC, diabetic control; HD-TFN, high-dose taxifolin; LD-TFN, low-dose taxifolin; n, total number of animals used in each group; NDC, nondiabetic control; SOD, superoxide dismutase

evaluate the effect of alloxan and treatment on the glycemic status of experimental animals, the levels of blood glucose (mg/dL) once in a week were measured in NDC-, DC-, ACB-, LD-TFN-, and HD-TFN-groups. As shown in Figure 1, we found that before the start of treatment, alloxan significantly increased the blood glucose level ($P < 0.001$) in all rats as compared to that of NDC rats. However, upon the start of treatment, we found that ACB, LD-TFN, and HD-TFN started to show the significant hypoglycemic effects at 15th day ($P < 0.001$) and 10th day ($P < 0.001$; Figure 1). At the end of the treatment period, it was found that ACB, LD-TFN, and HD-TFN exhibited significant ($P < 0.001$) hypoglycemic effects. Furthermore, we also observed that HD-TFN presented better hypoglycemic effects when compared with that of ACB ($P < 0.001$) and LD-TFN ($P < 0.05$) treated experimental rats.

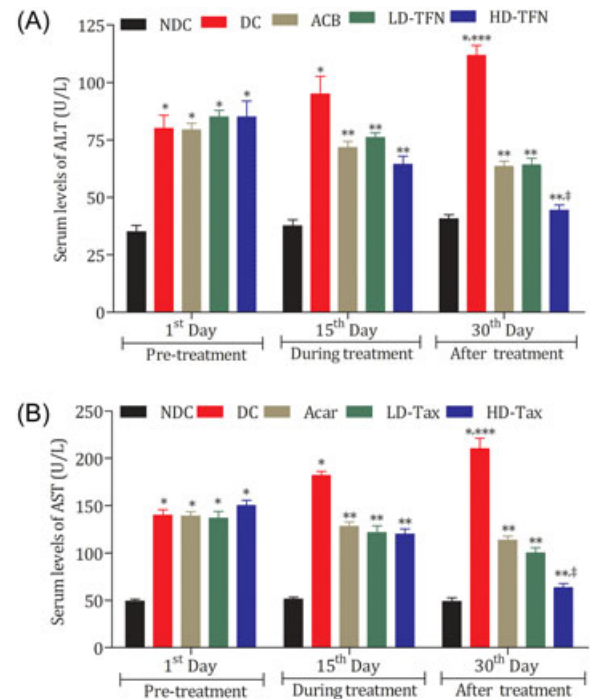


FIGURE 6 Effect of treatment on liver function biomarkers. To estimate the impact of alloxan and treatment on liver, the serum levels of AST (A) and ALT (B) were measured using their corresponding assay reagent kits at 1st, 15th, and last (30th) day of the treatment period. The level of significant difference was estimated by Bonferroni post-test using two-way ANOVA. * $P < 0.0001$ when compared with the NDC group. ** $P < 0.001$ when compared with the DC group at 15th and 30th day of the treatment period. † $P < 0.01$ when compared with the ACB group at the 30th day of the treatment period. *** $P < 0.001$ when compared with the DC group at the 30th day of the treatment period. ACB, acarbose; ALT, alanine aminotransferase; ANOVA, analysis of variance; AST, aspartate aminotransferase; DC, diabetic control; HD-TFN, high-dose taxifolin; LD-TFN, low-dose taxifolin; NDC, nondiabetic control

3.2 | Effect of treatment on amylase activity

α -amylase is one of the most important enzymes that is required for the breakdown of carbohydrates, and thus the level of glucose in the blood increases accordingly. Here, in our study, we also estimated the impact of treatment on serum levels of α -amylase. Before the start of treatment, alloxan exposure significantly ($P < 0.001$) elevated the serum levels of α -amylase (Figure 2). However, at the end of treatment, we found a highly significant difference ($P < 0.001$) between the serum levels of α -amylase in alloxan-induced experimental rats when compared with that of ACB-, LD-TFN-, and HD-TFN-treated experimental diabetic rats (Figure 2). At the end of treatment, we found that HD-TFN-treated experimental diabetic rats exhibited the lower levels of

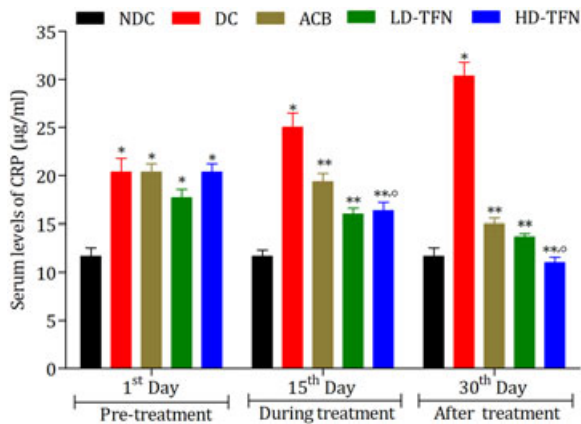


FIGURE 7 Effect of treatment on inflammation. To estimate the impact of alloxan and treatment (ACB, LD-TFN, and HD-TFN) on inflammation, the serum level of CRP was measured at 1st, 15th, and last (30th) day of the treatment period. The level of significant difference was estimated by Bonferroni post-test using two-way ANOVA. * $P < 0.001$ when compared with the NDC group. ** $P < 0.001$ when compared with the DC group. ^o $P < 0.01$ when compared with the ACB group. ACB, acarbose; ANOVA, analysis of variance; CRP, C-reactive protein; DC, diabetic control; HD-TFN, high-dose taxifolin; LD-TFN, low-dose taxifolin; NDC, nondiabetic control

α -amylase as compared to that of ACB ($P < 0.05$) and LD-TFN ($P < 0.001$) treated experimental rats.

3.3 | Effect of treatment on lipase activity

Lipase is a well-recognized enzyme for the metabolism and regulation of a normal lipid profile. Here, in our

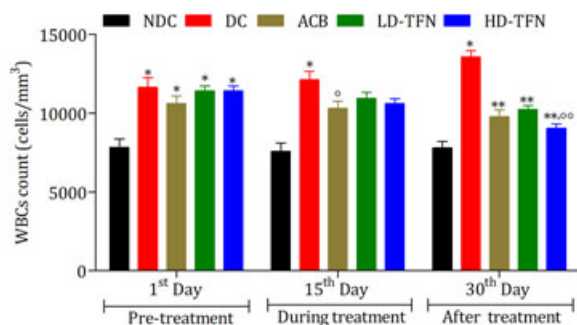


FIGURE 8 Effect of treatment on WBC count. To estimate the impact of alloxan and treatment (ACB, LD-TFN, and HD-TFN) on inflammation, WBC were counted at 1st, 15th, and last (30th) day of the treatment period. The level of significant difference was estimated by Bonferroni post-test using two-way ANOVA. * $P < 0.001$ when compared with the NDC group. ** $P < 0.001$ when compared with the DC group. ^o $P < 0.05$ when compared with the DC group. ^o $P < 0.01$ when compared with the ACB group. ACB, acarbose; ANOVA, analysis of variance; DC, diabetic control; HD-TFN, high-dose taxifolin; LD-TFN, low-dose taxifolin; NDC, nondiabetic control; WBC, white blood cell

study, we also estimated the impact of treatment on serum levels of lipase. Before the start of treatment, alloxan exposure significantly ($P < 0.001$) elevated the serum levels of lipase (Figure 3). However, at the end of treatment, we found a highly significant difference ($P < 0.001$) between the serum levels of lipase in alloxan-induced DC experimental rats when compared with that of ACB-, LD-TFN-, and HD-TFN-treated experimental diabetic rats (Figure 3). At the end of treatment, it was found that HD-TFN-treated experimental diabetic rats exhibited lower levels of lipase as compared to that of ACB ($P < 0.001$) and LD-TFN ($P < 0.001$) treated experimental rats.

3.4 | Effect of treatment on the lipid profile

The low levels of TC, TG, and LDL, and high levels of HDL in blood are considered as the normal lipid profile. Here, we also estimated the impact of treatment on the serum lipid profile. Before the start of the treatment, alloxan exposure significantly ($P < 0.001$) decreased the serum levels of HDL (Figure 4A), while the serum levels of TC, TG, and LDL were elevated (Figure 4B-D, respectively). At the end of treatment, we found a highly significant difference ($P < 0.001$) between the serum levels HDL, TC, TG, and LDL in alloxan-induced DC experimental rats when compared with that of ACB-, LD-TFN-, and HD-TFN-treated experimental diabetic rats (Figure 4). It was also found that HD-TFN-treated experimental diabetic rats exhibited the raised levels of HDL (Figure 4A), while the lowest levels of TC (Figure 4B), TG (Figure 4C), and LDL (Figure 4A) as compared to that of ACB ($P < 0.001$) and LD-TFN ($P < 0.05$) treated experimental rats.

3.5 | Effect of treatment on the anti-oxidant enzyme status

We also investigated the effect of treatment on the anti-oxidant enzyme status by measuring the serum levels of SOD and CAT using their assay reagent kits before, during, and at the end of the treatment period (Figure 5). As clearly seen in Figure 5A and B, alloxan significantly decreased the serum levels of SOD ($P < 0.0001$) and CAT ($P < 0.0001$), respectively, in alloxan-exposed experimental rats as compared to that of NDC experimental rats. However, at the end of the treatment, we found that HD-TFN did not significantly increase the serum levels of SOD (Figure 5A) and CAT (Figure 5B) at the 30th day of the treatment period as compared to that of ACB ($P < 0.001$) treated experimental diabetic rats.

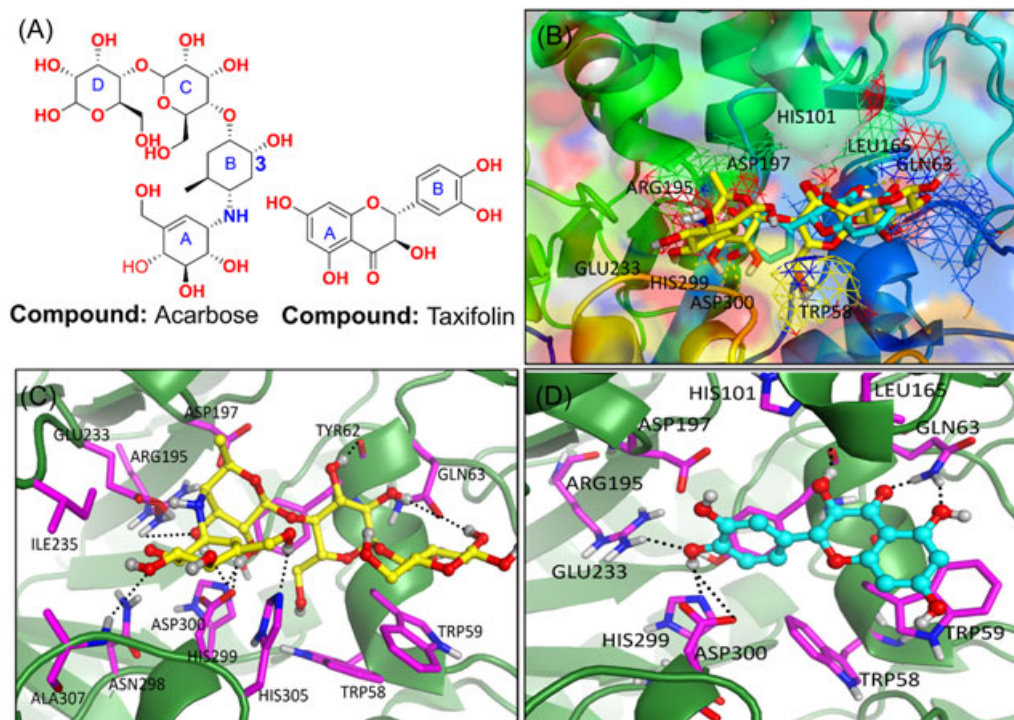


FIGURE 9 Docking results of acarbose and TFN. (A), Structural formulas of acarbose (ACB) and TFN. (B), Superimposition of the docked ligand ACB (yellow), TFN (cyan) in the main active site of α -amylase. Binding mode of (C) ACB/ α -amylase and (D) TFN/ α -amylase complexes. ACB, acarbose; TFN, taxifolin

3.6 | Effect of treatment on inflammation

To validate the therapeutic use of TFN against DM, the current study explored the anti-inflammatory potentials of TFN along with antihyperglycemic properties. For this, the serum levels of CRP were measured in DC-, ACB-, LD-TFN-, and HD-TFN-treated experimental diabetic rats. As shown in Figure 6, before the start of treatment, alloxan exposure significantly ($P < 0.001$) elevated the serum levels of CRP. However, at the end of treatment, we found a highly significant difference ($P < 0.001$) between the serum levels of CRP in alloxan-

induced DC experimental rats when compared to ACB-, LD-TFN-, and HD-TFN-treated experimental diabetic rats (Figure 6). It was found that HD-TFN-treated experimental diabetic rats exhibited better reduction in serum levels of CRP as compared to that of ACB-treated experimental rats ($P < 0.01$).

3.7 | Effect of treatment on the WBC count

To estimate the impact of alloxan and treatment (ACB, LD-TFN, and HD-TFN) on inflammation, the counts of

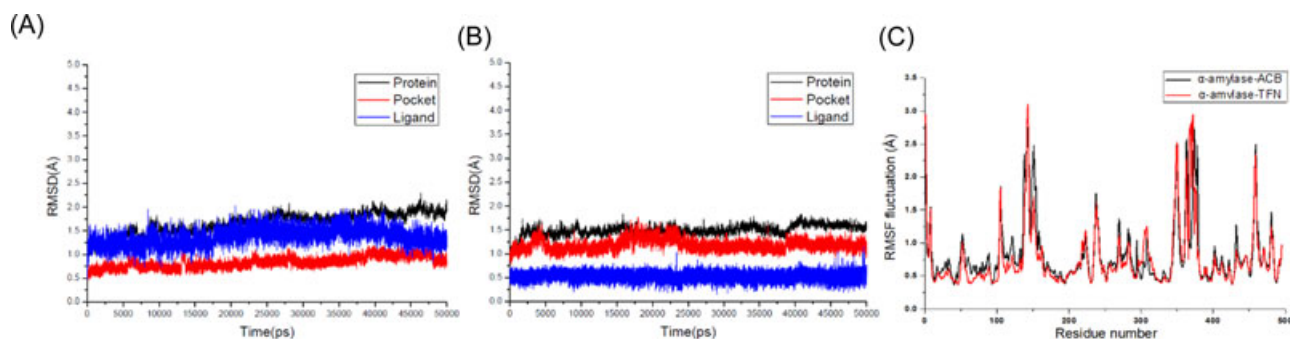


FIGURE 10 RMSDs of C- α atoms of protein. Backbone atoms of binding pocket (within 6.5 Å) and heavy atoms in the ligand for (A) acarbose- α -amylase, (B) taxifolin- α -amylase, and (C) RMSF of each residue of protein for the complex obtained from the crystal structure and all three α -amylase complexes obtained from 50 ns MD simulation. MD, molecular dynamics; RMSD, root-mean-square deviation; RMSF, root-mean-square fluctuation

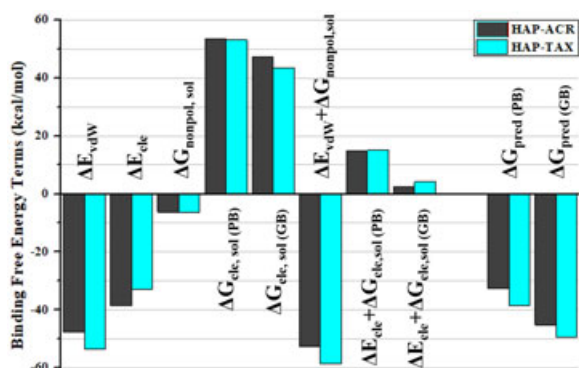


FIGURE 11 Comparison between binding-free energy in terms of α -amylase bonded with acarbose (in black) and taxifolin (in cyan)

WBCs were made at 1st, 15th, and 30th day of the treatment period. It was noticed that after exposure to alloxan and before the start of the treatment, there was an elevation in the normal count of WBCs of all alloxan-exposed groups when compared with that of the NDC group (Figure 7). However, it was found that HD-TFN-treated experimental diabetic rats exhibited better reduction in WBCs count even when compared to that of ACB-treated experimental rats ($P < 0.01$).

3.8 | Effect of treatment on liver function biomarkers

We measured the serum levels of AST and ALT before, during, and at the end of the treatment period (1st, 15th, and 30th day) and their level of significant difference was estimated by Bonferroni post-test using two-way analysis of variance (ANOVA; Figure 8). We found that alloxan significantly increased ($P < 0.0001$) the serum levels of both enzymes (AST and ALT) as compared to their NDC rats (Figure 8A and 8 B). But, when the treatment was started, we found that LD-TFN ($P < 0.001$) and HD-TFN ($P < 0.001$) ameliorated the adverse effects of alloxan on the liver by significantly decreasing the serum levels of liver function biomarkers (AST and ALT) as compared to that of DC experimental rats. At the end of the treatment period, we also noticed that LD-TFN ($P < 0.001$) and HD-TFN ($P < 0.001$) significantly counterfeited the side effects of alloxan on liver function biomarkers (AST and ALT) as compared to that of ACB-treated experimental rats (Figure 8).

3.9 | Molecular docking and molecular dynamics simulation

In the present work, molecular docking studies were performed to reveal the key molecular interactions

responsible for the difference in binding affinities of studied ligands toward target protein. The best-docked poses were selected based on the cumulative score (C -score) as depicted in Table S1. The docking scores of ACB and TFN for α -amylase are 6.24 and 6.89, respectively, which indicate that TFN has a relatively higher binding affinity toward α -amylase than ACB. Furthermore, these top-ranked docking poses (Figure 9) were saved for each compound and graphically viewed to identify the ligand–protein interactions responsible for the difference in binding affinity. As depicted in Figure 9B, both ligands acquired similar mode of interaction within the active site of α -amylase, where they can make several H-bond interactions with surrounding residues. The graphical analysis shows that Trp58, trp59, Tyr62, Gln63, Hie101, ALeu162, Leu165, Arg195, Asp197, Ala198, Glu233, Ile235, Phe256, Hie299, Asp300, Hie305, Gly306, and Ala307 are the most important residues present at the active site. The best possible interacting model of ACB with α -amylase is displayed in Figure 9C. The docked model of ACB reveals that the compound occupies the major area of pocket and make 11 H-bond interactions with surrounding residues such as Tyr62, Gln63, Arg195, Glu233, Hie299, Asp300, Hie305, and Ala307. The $-NH$ group, which is located between the ring A and ring B, and hydroxyl group located at C-3 of ring B act as H-bond donor to form 2H bonds with the carbonyl function of Glu233 and Asp300 (Figure 9C). Interestingly, Glu233 and Asp300 are critical because of their key role in hydrolysis of glycosidic bonds of carbohydrates. The involvement of these residues has already been reported in making key interactions with myricetin and ethyl caffeate,³⁴ which supports the accuracy of docking results of our study.

To elucidate the interaction mode of TFN with α -amylase, the top-ranked docked pose of the TFN– α -amylase complex was also critically analyzed (Figure 9C). The docking results show that most residues contributing toward ACB binding to α -amylase also have favorable interactions with TFN. However, unlike ACB– α -amylase system, Hie305 and Ala307 of α -amylase are unable to interact with TFN, as TFN is relatively smaller in size than ACB. As shown in Figure 9C, TFN was able to establish at least eight H-bond interaction with surrounding residues including key residues Glu233 and Asp300 in donor acceptor motif. Furthermore, ring-A and -B of TFN extend in the opposite direction within ligand binding cleft of α -amylase, where they were able to establish two additional π – π interaction with benzene rings of Trp59 and Tyr62 of α -amylase (Figure 9C and Figure S2), whereas no such interaction was observed in the case of an ACB– α -amylase complex system, as ACB lacks any aromatic ring in its structure (Figure 9,10B).

Since ACB established greater number of H-bond interactions, the better binding affinity of TFN to α -amylase than ACB suggests that apart from H-bonding interaction other nonbonding interactions also play a critical role toward the binding of a ligand with a receptor under an energetically favored condition. Thus, these variations in a ligand–receptor interaction pattern could account for the higher α -amylase inhibitory potency of TFN than ACB.

Although docking analysis can provide an acceptable binding mode, the solvent, temperature, and pressure effects could not be taken into account. Therefore, docking results were postprocessed with more reliable MD simulations to describe the dynamical behavior of complex at an atomic level by flexibly and firmly treating a ligand–receptor complex. Moreover, it also allows to calculate the binding-free energies using an implicit MMGB (PB) SA approach, which provides an accurate ranking of potential ligands binding to the target protein. To inspect the dynamic stability of studied complex systems, the fluctuation of root-mean-square deviation (RMSD) of backbone atoms was examined over 50 ns of MD trajectories. As illustrated in Figure 10A and 10 B, each system achieved equilibrium rapidly after some initial fluctuations, which indicate a stable conformation for a docked structure. Figure 10A and 10B also illustrates the RMSD of the ligand (in blue) in the active site, where RMSD of ACB reaches at 1.2 Å during 20 to 30 ns, then level off to 0.8 Å in the following 20 ns, whereas the RMSD of ACB remains constant at 0.5 Å throughout the simulation, thus indicating the stable conformation of TFN in its active site. These results captured our attention toward the fact that ACB exhibit a relatively larger structure than TFN. Therefore, ACB may switch between two kinds of conformations in the binding site, which may induce changes in the length and the number of the H bonds with surrounding residues. These conformational fluctuations were further confirmed by overlaying the coordinates of representative MD-simulated snapshot over the initial confirmation (Figure S3). These findings also explain why the TFN demonstrates higher binding affinity in TFN– α -amylase complex over ACB– α -amylase. Figure 10C depicts the analyses of root-mean-square fluctuation (RMSF) against the residue number for both ligand–receptor complexes. The protein structures of both complexes display a similar pattern of RMSF. The results indicate that higher fluctuations of the residues in the TFN– α -amylase system as compared to the ACB– α -amylase system. The ligand binding site residues including Trp58, trp59, Tyr62, Gln63, Hie101, ALeu162, Leu165, Arg195, Asp197, Ala198, Glu233, Ile235, Phe256, Hie299, Asp300, Hie305, Gly306, and Ala307 display greater

conformational drift for the TFN– α -amylase system than that for the ACB-bound system. Overall, these analyses for binding stabilization further reinforce the accuracy of molecular docking and experimental results.

The binding-free energies of both ACB- and TFN-bonded systems were computed using an MMGB/PBSA approach. The results are plotted and summarized in Figure 11 and Table S2, respectively. These results show a noticeable difference of computed binding affinities for ACB ($\Delta G_{\text{pred (GB)}} = -45.19 \text{ kcal}\cdot\text{mol}^{-1}$) and TFN ($\Delta G_{\text{pred (GB)}} = -49.48 \text{ kcal}\cdot\text{mol}^{-1}$). Although the difference in binding-free energies is not very high but sufficiently reflect the fact that TFN exhibits greater binding affinity toward α -amylase than ACB. Consequently, these results are also in agreement with molecular docking and experiment results. To identify the key driving forces responsible for higher binding affinities of TFN, total binding-free energy was further decomposed into independent binding-free energy components (Figure 11 and Table S2). As shown in Figure 11, the van der Waals interactions and the nonpolar solvation contribution arising either from aromatic interactions or the burial of the hydrophobic moieties (ring A and B) represent the favorable binding-free energies for TFN ($-53.62 \text{ kcal}\cdot\text{mol}^{-1}$) over ACB ($-47.64 \text{ kcal}\cdot\text{mol}^{-1}$). Although variations in electrostatic interactions also make noticeable differences in binding affinity of the ACB-bonded system (Figure 11), the decrease of the van der Waals contribution may be responsible for the decrease in binding affinity of ACB. Hence, it might be proposed that the higher binding affinities of inhibitor TFN are mainly dominated by the van der Waals and nonpolar solvation-free energies along with electrostatic and H-bond interaction.

4 | DISCUSSION

Hyperglycemia is one of the main parameters of T2DM, which is a metabolic disorder and is rapidly prevailing globally. The use of synthetic antidiabetic agents that are commercially available is usually associated with some unavoidable adverse effects.^{11,35} Due to these adverse effects, the use of traditional plant-oriented medicinal compounds has gained considerable attention.^{8,15,36–38} Among various therapeutic strategies for the treatment of hyperglycemia including postprandial hyperglycemia, inhibition of the activity of carbohydrate digestive enzymes like α -amylase and/or glucosidase can be a useful option.³⁹ Inhibition of glucose absorption and metabolism has proven to ameliorate the hyperglycemia.⁷ In this study, ACB was used as a standard of the α -amylase inhibitor for comparative analysis. ACB derived from

microorganism and along with other synthetic potent α -amylase inhibitors like miglito has been recognized for causing adverse effects like flatulence, bloating, allergy, and liver injury.⁴⁰ Hence, the work has been focusing on exploring the plant-based compounds for their potential as inhibitors of carbohydrate-metabolizing enzyme α -amylase so to have maximum therapeutic effects with minimum untoward effects.^{41,42} The current work showed a therapeutic potential of a well-known flavonoid, TFN, against the inhibition of α -amylase enzyme, and thus helps to reduce the hyperglycemia (Figure 1) and ameliorates deleterious parameters associated with DM. Both low and high doses of TFN showed a rapid reduction in the blood glucose level in alloxan-induced diabetic rats (Figure 1). The probable effect could be reduction in insulin resistance or increase in the release of insulin from β -cells of pancreatic islets. However, if this hyperglycemia needs to be reverted, inhibition of carbohydrate-digesting enzyme, which contributes in increasing the blood glucose level, is an effective therapeutic approach.⁴³ Interestingly, in an *in vivo* study, we found that TFN was capable of reducing the activity of α -amylase in a dose-dependent manner to a better extent when compared with that of standard drug ACB (Figure 2), and hence, we found the subsequent reduction in hyperglycemia of the same treated group (Figure 1). This correlation supports the role of α -amylase and inhibitory effect of TFN on α -amylase for decreasing the blood sugar level. In addition, to the best of our knowledge, we have for the very first time evaluated the role of TFN in inhibition of α -amylase *in vivo* and *in silico* determination of its binding energy with target enzyme.

Alteration in the serum level of the lipid profile is associated with the increased level of lipase enzyme during the pathogenesis of DM.⁴⁴ Absorption of fats are recognized to be decreased by the inhibition of a key enzyme, that is, lipase.⁴⁵ Correspondingly, we also found that treatment of alloxan-induced diabetic rats with TFN reduced the serum level of lipase enzyme (Figure 3) in a significant manner that was expected to reduce the absorption of fats into the bloodstream. Previously, it has been shown that the increased serum level of TC, TG, and LDL in diabetic rats is associated with the altered serum lipase level.⁴⁶ Remarkably, as anticipated, the treatment of TFN provided the reduction in serum levels of TC, TG, and LDL, which were otherwise found to be elevated in nontreated alloxan-induced diabetic rats (Figure 3). This result is in line with other work done by evaluating the role of flavonoids on the lipid profile.⁴⁷ This reduction in the level of lipids in our study could be in part due to inhibition of lipase enzyme by TFN.

Among these deleterious parameters, generation of ROS is one of the major factors associated to be increased along with the progression of hyperglycemia and its complications.⁴⁸⁻⁵¹ Among the risk factors of diabetes, generation of ROS is considered to play a crucial role in the development and progression of DM. They are also known for their damaging effects on the islets of pancreas.^{50,52} Flavonoids have shown to have anti-oxidant activities through various mechanisms of actions^{15,53,54}; however, the anti-oxidant potential of TFN in diabetic rats has not been evaluated in detail. Hence, this study also provides the evidence of potential anti-oxidant property of TFN during DM. This was observed by the recovery in the serum levels of anti-oxidant enzymes (SOD and CAT) in diabetic rats after their treatment with LD-TFN and HD-TFN (Figure 4A and B). TFN has also previously been reported by inhibiting the hyperglycemia-induced apoptosis by overturning the oxidative stress.⁵⁵ Oxidative stress due to induction of ROS and/or reduction in the activities of anti-oxidant enzymes may play an important role in the pathogenesis of DM and its associated complications.⁴⁹ In our study, we found a remarkable decrease in the serum levels of SOD and CAT (Figure 5A and 5B) in alloxan-induced diabetic rats, but TFN significantly increased the serum levels of SOD and CAT in a dose-dependent manner in a better way as compared to that of ACB-treated diabetic rats (Figure 5). The anti-oxidant potential of TFN reported in our study follows the same pattern as was observed previously.⁵⁵

It has been well documented that inflammation plays a key role during the pathogenesis of T2DM and has now been considered as one of the main risk factors for the development of insulin resistance and pathogenesis of T2DM.^{48,56-58} Dietary polyphenols have been reported to exhibit the anti-inflammatory properties in various types of diseases notably.^{15,53} Previously, it has been reported that elevated levels of CRP reported during DM have been considered as an inflammatory biomarker for the prediction of DM. Similarly, to validate the anti-inflammatory potential of TFN in alloxan-induced DM in experimental rats, the serum levels of CRP were measured (Figure 7). TFN also showed its anti-inflammatory potential in alloxan-induced DM that was estimated by measuring the serum level of CRP. Here, we found a highly significant difference between the serum levels of CRP in alloxan-induced diabetic experimental rats and TFN-treated experimental diabetic rats (Figure 7). Moreover, TFN exhibited better anti-inflammatory effects when compared with that of ACB (Figure 7). Moreover, we also found that alloxan significantly decreased the total counts of WBCs (Figure 8), which indicate the induction of inflammation in diabetic rats, but at the end of treatment period,

TFN significantly decreased the WBCs count as compared to that of nontreated alloxan-induced diabetic rats (Figure 8). These results are found to be in line with the recent study in which similar findings have also been reported.⁵⁹ This clearly indicates that TFN reduced the process of inflammation that was initiated after alloxan exposure partly by hyperglycemia and due to induction of oxidative stress.

In addition, the *in silico* studies of TFN and ACB were performed using molecular docking and MD simulation to compare their binding affinities and energies with the target enzyme, α -amylase. A combined molecular docking and MD simulation approaches were applied to reveal the key structural basis responsible for high inhibitory potency of TFN than ACB against α -amylase. The results indicate that molecular docking and MD simulations results are in a strong correlation with experimental results. The MD simulation and MM/PBSA calculations further rationalized the reasonable binding mode of ACB- and TFN-bound complexes, and the π - π interactions were identified as key driving forces to be responsible for higher binding affinities of TFN than ACB.


5 | CONCLUSION

We aimed to investigate the inhibitory effects of TFN on α -amylase activity through assessment of its therapeutic potential in diabetic rat models and its enzyme binding potential through the MD simulation and computational tools. The key findings of this study indicate that TFN is a potent inhibitor of α -amylase as compared to that of ACB and it has the ability to prevent the postprandial hyperglycemia. Moreover, it has the potential to exhibit its anti-inflammatory and anti-oxidative effects during the pathogenesis of T2DM. In addition to the significant outcomes obtained during *in vivo* experiments, molecular docking results also revealed that the π - π interaction in the TFN- α -amylase complex system imparted the better binding affinity of TFN for α -amylase as compared to that of ACB.

CONFLICTS OF INTEREST

The authors declare that there are no conflicts of interest.

ORCID

Muhammad Sajid Hamid Akash  <http://orcid.org/0000-0002-9446-5233>

REFERENCES

1. Akash MSH, Rehman K, Chen S. Role of inflammatory mechanisms in pathogenesis of type 2 diabetes mellitus. *J Cell Biochem*. 2013;114(3):525-531.
2. Akash MSH, Rehman K, Sun H, Chen S. Interleukin-1 receptor antagonist improves normoglycemia and insulin sensitivity in diabetic Goto-Kakizaki-rats. *Eur J Pharmacol*. 2013;701(1-3):87-95.
3. Akash MSH, Rehman K, Sun H, Chen S. Sustained delivery of IL-1Ra from PF127-gel reduces hyperglycemia in diabetic GK-rats. *PLoS One*. 2013;8(2):e55925.
4. Ceriello A. Postprandial hyperglycemia and diabetes complications: is it time to treat? *Diabetes*. 2005;54(1):1-7.
5. Ceriello A, Esposito K, Piconi L, et al. Oscillating glucose is more deleterious to endothelial function and oxidative stress than mean glucose in normal and type 2 diabetic patients. *Diabetes*. 2008;57(5):1349-1354.
6. Kato A, Minoshima Y, Yamamoto J, Adachi I, Watson AA, Nash RJ. Protective effects of dietary chamomile tea on diabetic complications. *J Agric Food Chem*. 2008;56(17):8206-8211.
7. Bhandari MR, Jong-Anurakkun N, Hong G, Kawabata J. α -Glucosidase and α -amylase inhibitory activities of Nepalese medicinal herb Pakhanbhed (*Bergenia ciliata*, Haw.). *Food Chem*. 2008;106(1):247-252.
8. Rehman K, Saeed K, Munawar SM, Akash MSH. Resveratrol regulates hyperglycemia-induced modulations in experimental diabetic animal model. *Biomed Pharmacother*. 2018;102:140-146.
9. Grabitske HA, Slavin JL. Gastrointestinal effects of low-digestible carbohydrates. *Crit Rev Food Sci Nutr*. 2009;49(4):327-360.
10. Gholamhoseinian A, Fallah H, Sharifi far F. Inhibitory effect of methanol extract of *Rosa damascena* Mill. flowers on alpha-glucosidase activity and postprandial hyperglycemia in normal and diabetic rats. *Phytomedicine*. 2009;16(10):935-941.
11. Akash MSH, Shen Q, Rehman K, Chen S. Interleukin-1 receptor antagonist: a new therapy for type 2 diabetes mellitus. *J Pharm Sci*. 2012;101(5):1647-1658.
12. Rosak C, Mertes G. Critical evaluation of the role of acarbose in the treatment of diabetes: patient considerations. *Diabetes Metab Syndr Obes*. 2012;5:357-367.
13. Tahrani AA, Piya MK, Kennedy A, Barnett AH. Glycaemic control in type 2 diabetes: targets and new therapies. *Pharmacol Ther*. 2010;125(2):328-361.
14. Li JM, Che CT, Lau CBS, Leung PS, Cheng CHK. Inhibition of intestinal and renal Na⁺-glucose cotransporter by naringenin. *Int J Biochem Cell Biol*. 2006;38(5-6):985-995.
15. Rehman K, Al-Gubory KH, Laher I, Akash MSH. Dietary polyphenols in the prevention and treatment of diabetes mellitus. In: Al-Gubory KH, Laher I, eds. *Nutritional Anti-oxidant Therapies: Treatments and Perspectives*. Cham: Springer International Publishing; 2017: pp.377-395.
16. Weidmann AE. Dihydroquercetin: more than just an impurity? *Eur J Pharmacol*. 2012;684(1-3):19-26.
17. Haraguchi H, Ohmi I, Fukuda A, et al. Inhibition of aldose reductase and sorbitol accumulation by astilbin and taxifolin dihydroflavonols in *Engelhardtia chrysolepis*. *Biosci Biotechnol Biochem*. 1997;61(4):651-654.
18. Vladimirov YA, Proskurnina EV, Demin EM, et al. Dihydroquercetin (taxifolin) and other flavonoids as inhibitors of free

- radical formation at key stages of apoptosis. *Biochemistry*. 2009;74(3):301-307.
19. Wang S, Griffiths G, Midgley CA, et al. Discovery and characterization of 2-anilino-4-(thiazol-5-yl) pyrimidine transcriptional CDK inhibitors as anticancer agents. *Chem Biol*. 2010;17(10):1111-1121.
 20. Tan T-C, Mijts BN, Swaminathan K, Patel BKC, Divne C. Crystal structure of the polyextremophilic α -amylase AmyB from *Halothermothrix orenii*: details of a productive enzyme-substrate complex and an N domain with a role in binding raw starch. *J Mol Biol*. 2008;378(4):852-870.
 21. Maurus R, Begum A, Williams LK, et al. Alternative catalytic anions differentially modulate human α -amylase activity and specificity. *Biochemistry*. 2008;47(11):3332-3344.
 22. Akash MSH, K. K, A. A. Tumor necrosis factor- α : role in development of insulin resistance and pathogenesis of type 2 diabetes mellitus. *J Cell Biochem*. 2018;119(1):105-110.
 23. Jain AN. Surflex: fully automatic flexible molecular docking using a molecular similarity-based search engine. *J Med Chem*. 2003;46(4):499-511.
 24. Jain AN. Scoring noncovalent protein-ligand interactions: a continuous differentiable function tuned to compute binding affinities. *J Comput Aided Mol Des*. 1996;10(5):427-440.
 25. Jain AN. Surflex: fully automatic flexible molecular docking using a molecular similarity-based search engine. *J Med Chem*. 2003;46(4):499-511.
 26. Case D, Betz R, Botello-Smith W, et al. *AMBER 16*. San Francisco, CA: University of California; 2016.
 27. Duan Y, Wu C, Chowdhury S, et al. A point-charge force field for molecular mechanics simulations of proteins based on condensed-phase quantum mechanical calculations. *J Comput Chem*. 2003;24(16):1999-2012.
 28. Berendsen HJ, Postma Jv, van Gunsteren WF, DiNola A, Haak J. Molecular dynamics with coupling to an external bath. *J Chem Phys*. 1984;81(8):3684-3690.
 29. Becke AD. Density-functional thermochemistry. III. The role of exact exchange. *J Chem Phys*. 1993;98(7):5648-5652.
 30. Jorgensen WL, Chandrasekhar J, Madura JD, Impey RW, Klein ML. Comparison of simple potential functions for simulating liquid water. *J Chem Phys*. 1983;79(2):926-935.
 31. Chohan TA, Chen J-J, Qian H-Y, Pan Y-L, Chen J-Z. Molecular modeling studies to characterize N-phenylpyrimidin-2-amine selectivity for CDK2 and CDK4 through 3D-QSAR and molecular dynamics simulations. *Mol BioSyst*. 2016;12(4):1250-1268.
 32. Ryckaert J-P, Ciccotti G, Berendsen HJC. Numerical integration of the cartesian equations of motion of a system with constraints: molecular dynamics of n-alkanes. *J Comput Phys*. 1977;23(3):327-341.
 33. Fogolari F, Brigo A, Molinari H. Protocol for MM/PBSA molecular dynamics simulations of proteins. *Biophys J*. 2003; 85(1):159-166.
 34. Williams LK, Li C, Withers SG, Brayer GD. Order and disorder: differential structural impacts of myricetin and ethyl caffeate on human amylase, an antidiabetic target. *J Med Chem*. 2012; 55(22):10177-10186.
 35. Shafiee G, Mohajeri-Tehrani M, Pajouhi M, Larijani B. The importance of hypoglycemia in diabetic patients. *J Diabetes Metab Disord*. 2012;11:17-17.
 36. Tsai HY, Ho CT, Chen YK. Biological actions and molecular effects of resveratrol, pterostilbene, and 3'-hydroxypterostilbene. *J Food Drug Anal*. 2017;25(1):134-147.
 37. Akash MSH, Rehman K, Chen S. Spice plant *Allium cepa*: dietary supplement for treatment of type 2 diabetes mellitus. *Nutrition*. 2014;30(10):1128-1137.
 38. Akash MSH, Rehman K, Chen S. Effects of coffee on type 2 diabetes mellitus. *Nutrition*. 2014;30(7-8):755-763.
 39. Hamden K, Keskes H, Belhaj S, Mnafigui K, Feki A, Allouche N. Inhibitory potential of omega-3 fatty and fenugreek essential oil on key enzymes of carbohydrate-digestion and hypertension in diabetes rats. *Lipids Health Dis*. 2011;10:226.
 40. Charpentier G, Riveline JP, Varroud-Vial M. Management of drugs affecting blood glucose in diabetic patients with renal failure. *Diabetes Metab*. 2000;26(Suppl 4):S73-S85.
 41. Heo SJ, Hwang JY, Choi JI, Han JS, Kim HJ, Jeon YJ. Diploretohydroxycarmalol isolated from *Ishige okamurae*, a brown algae, a potent α -glucosidase and α -amylase inhibitor, alleviates postprandial hyperglycemia in diabetic mice. *Eur J Pharmacol*. 2009;615(1-3):252-256.
 42. Kim KY, Nam KA, Kurihara H, Kim SM. Potent α -glucosidase inhibitors purified from the red alga *Grateloupia elliptica*. *Phytochemistry*. 2008;69(16):2820-2825.
 43. Krentz AJ, Bailey CJ. Oral antidiabetic agents: current role in type 2 diabetes mellitus. *Drugs*. 2005;65(3):385-411.
 44. Burski K, Ueland T, Maciejewski R. Serum amylase activity disorders in the course of experimental diabetes in rabbits. *Veterinarni Med*. 2004;49(6):197-200.
 45. Hamden K, Keskes H, Elgomdi O, Feki A, Alouche N. Modulatory effect of an isolated triglyceride from fenugreek seed oil on α -amylase, lipase and ACE activities, liver-kidney functions and metabolic disorders of diabetic rats. *J Oleo Sci*. 2017;66(6):633-645.
 46. Aloulou A, Hamden K, Elloumi D, et al. Hypoglycemic and antilipidemic properties of kombucha tea in alloxan-induced diabetic rats. *BMC Complement Altern Med*. 2012;12:63.
 47. Saravanan G, Ponmurugan P, Deepa MA, Senthilkumar B. Anti-obesity action of gingerol: effect on lipid profile, insulin, leptin, amylase and lipase in male obese rats induced by a high-fat diet. *J Sci Food Agric*. 2014;94(14): 2972-2977.
 48. Akash MSH, Rehman K, Chen S. Role of inflammatory mechanisms in pathogenesis of type 2 diabetes mellitus. *J Cell Biochem*. 2013;114(3):525-531.
 49. Khullar M, Al-Shudiefat AARS, Ludke A, Binopal G, Singal PK. Oxidative stress: a key contributor to diabetic cardiomyopathy. *Can J Physiol Pharmacol*. 2010;88(3):233-240.
 50. Rehman K, Akash MSH. Mechanisms of inflammatory responses and development of insulin resistance: how are they interlinked? *J Biomed Sci*. 2016;23(1):87.
 51. Rehman K, Akash MSH. Mechanism of generation of oxidative stress and pathophysiology of type 2 diabetes mellitus: how are they interlinked? *J Cell Biochem*. 2017;118 (11):3577-3585.
 52. Rani V, Deep G, Singh RK, Palle K, Yadav UCS. Oxidative stress and metabolic disorders: pathogenesis and therapeutic strategies. *Life Sci*. 2016;148:183-193.

53. Rehman K, Akash MSH. Nutrition and diabetes mellitus: how are they interlinked? *Crit Rev Eukaryot Gene Expr.* 2016; 26(4):317-332.
54. Zhang H, Tsao R. Dietary polyphenols, oxidative stress and antioxidant and anti-inflammatory effects. *Curr Opin Food Sci.* 2016;8:33-42.
55. Sun X, Chen R, Yang Z, et al. Taxifolin prevents diabetic cardiomyopathy in vivo and in vitro by inhibition of oxidative stress and cell apoptosis. *Food Chem Toxicol.* 2014;63:221-232.
56. Akash MSH, Rehman K, Liaqat A. Tumor necrosis factor-alpha: role in development of insulin resistance and pathogenesis of type 2 diabetes mellitus. *J Cell Biochem.* 2018;119(1):105-110.
57. Rehman K, Akash MSH, Alina Z. Leptin: a new therapeutic target for treatment of diabetes mellitus. *J Cell Biochem.* 2017;119:5016-5027. <https://doi.org/10.1002/jcb.26580>
58. Rehman K, Akash MSH, Liaqat A, Kamal S, Qadir MI, Rasul A. Role of interleukin-6 in development of insulin resistance and type 2 diabetes mellitus. *Crit Rev Eukaryot Gene Expr.* 2017; 27(3):229-236.
59. Arutyunyan TV, Korystova AF, Kublik LN, Levitman MK, Shaposhnikova VV, Korystov YN. Taxifolin and fucoidin

abolish the irradiation-induced increase in the production of reactive oxygen species in rat aorta. *Bull Exp Biol Med.* 2016; 160(5):635-638.

SUPPORTING INFORMATION

Additional supporting information may be found online in the Supporting Information section at the end of the article.

How to cite this article: Rehman K, Chohan TA, Waheed I, Gilani Z, Akash MSH. Taxifolin prevents postprandial hyperglycemia by regulating the activity of α -amylase: Evidence from an in vivo and in silico studies. *J Cell Biochem.* 2018;1-14. <https://doi.org/10.1002/jcb.27398>